INTERNATIONAL JOURNAL OF HYDROGEN ENERGY 35 (2010) 4420–4427

Available at www.sciencedirect.com

ScienceDirect

journal homepage: www.elsevier.com/locate/he

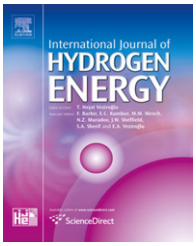

Synthesis of highly-ordered TiO_2 nanotubes for a hydrogen sensor

Erdem Şennik [a], *Zeliha Çolak* [a], *Necmettin Kılınç* [a], *Zafer Ziya Öztürk* [a,b,*]

[a] *Gebze Institute of Technology, Faculty of Science, Dept. of Phys., 41400 Gebze, Kocaeli, Turkey*
[b] *TÜBİTAK-Marmara Research Center, Materials Institute, 41470 Gebze, Kocaeli, Turkey*

ARTICLE INFO

Article history:
Received 11 September 2009
Received in revised form
10 January 2010
Accepted 24 January 2010
Available online 5 March 2010

Keywords:
TiO_2 nanotubes
Anodic oxidation
Hydrogen sensor
Nanotubes
Titania

ABSTRACT

Highly-ordered, vertically oriented TiO_2 nanotubes are synthesized, and their hydrogen sensing properties are investigated. Self-organized TiO_2 nanotube arrays are grown by anodic oxidation of a titanium foil in an aqueous solution that contains 1 wt% hydrofluoric acid at 20 °C. We use a potential ramp at a rate of 100 mV s^{-1}, increasing from the initial open-circuit potential (OCP) to 20 V, and this final potential of 20 V is then held constant during the anodization process. The fabricated TiO_2 nanotubes are approximately 1 μm in length and 90 nm in diameter. For the sensor measurements, two platinum pads are used as electrodes on the TiO_2 nanotube arrays. The hydrogen sensing characteristics of the sensor are analyzed by measuring the sensor responses $((I - I_0)/I_0)$ in the temperature interval of 20–150 °C. We find that the sensitivity of the sensor is approximately 20 for 1000 ppm H_2 exposure at room temperature, and increases with increasing temperature. The sensing mechanism of the TiO_2 nanotube sensor could be explained with chemisorption of H_2 on the highly active nanotube surface.

1. Introduction

Hydrogen has numerous applications in industry, such as chemical production, fuel cell technology, and rocket engines [1]. However, the flammable and explosive properties of hydrogen gas make its detection an important issue [2]. Therefore, today a wide range of investigations are being carried out toward the development of highly sensitive, compact, low-cost, and reliable hydrogen sensors [3]. In order to overcome the disadvantages of commercially available hydrogen sensors [4], different detection principles, methods, and materials have been utilized to manufacture sensors during the last few decades. The basic categories of sensors include catalytic sensors, electrochemical sensors, resistive palladium and palladium alloy sensors, field effect transistors, Schottky diodes, and semiconductor metal oxide sensors [5–11].

Metal oxide films have been playing an increasingly important role in the last few years as sensing materials for various gases [9]. TiO_2 based gas sensors have been widely used because of their inert surface properties and high sensing abilities [12,13]. Recently, many nanotechnological approaches have been employed to enlarge the surface area of TiO_2 without increasing the device dimensions [14,15]. Highly-ordered TiO_2 nanotubes were first synthesized using an anodization process by Grimes et al., using hydrofluoric acid (HF) electrolyte [16]. Thereafter, further studies succeeded in controlling and extending the nanotube morphology [17], the length and pore size [18], and the wall thickness [19]. The choice of electrolyte plays a critical role in determining the resultant nanotube array. Several electrolytes, such as HF/H_2O [16,20], $HF/H_2SO_4/H_2O$ [21], NH_4F/H_2SO_4 [22], $KF/NaF/H_2O$ [18], $NH_4F/(NH_4)_2SO_4/H_2O$ [23], and fluoride-free HCl aqueous

---

[*] *Corresponding author* at: Gebze Institute of Technology, Faculty of Science, Department of Physics, 41400 Gebze, Kocaeli, Turkey.
E-mail address: zozturk@gyte.edu.tr (Z.Z. Öztürk).

0360-3199/$ – see front matter © 2010 Professor T. Nejat Veziroglu. Published by Elsevier Ltd. All rights reserved.
doi:10.1016/j.ijhydene.2010.01.100

electrolyte [24], were used to fabricate TiO_2 nanotube arrays. Long nanotube arrays up to 1000 μm were produced in fluoride ion containing baths in combination with a variety of nonaqueous organic polar electrolytes, including dimethyl sulfoxide, formamide, ethylene glycol, and N-methylformamide [25–27]. The geometrical features of TiO_2 nanotube arrays are controlled by a variety of anodization parameters (potential, time, and temperature) and a variety of electrolyte parameters (composition, pH, viscosity and primarily conductivity). The aqueous HF electrolyte was used to fabricate TiO_2 nanotube arrays with limited tube lengths of up to 500 nm because of the high H_2O content of the electrolytes [16,20]. In this work, we have constructed TiO_2 nanotube arrays that are approximately 1 μm in length with the aqueous HF electrolyte, and potential ramping from the open-circuit potential to 20 V in 100 $mV\,s^{-1}$ steps and then holding this potential constant for approximately 45 min.

TiO_2 nanotube arrays have a wide range of applications in areas such as photoelectrochemical materials, dye-sensitized solar cells, hydrogen (H_2) sensors, oxygen (O_2) sensors, biosensing and biomedical applications, and catalyst support because of their various functional properties [28–31]. For the H_2 sensor at room temperature, undoped micrometer-length TiO_2 nanotube arrays prepared by anodization of Ti foil in an electrolyte containing potassium fluoride, sodium hydrogen sulfate monohydrate, and sodium citrate tribasic dihydrate demonstrate an unprecedented change in electrical resistance, of 8.7 orders of magnitude [32]. In previous works, the H_2 sensing properties of TiO_2 nanotube arrays were studied in terms of the nanotube length, the catalysis coating electrode, and the carrier gas. The highest sensitivity was observed for micrometer-length TiO_2 nanotubes with catalysis (Pd, or Pt) nanofilm coating and using dry air as carrier gas. The responses of TiO_2 nanotube arrays that are prepared with an aqueous HF electrolyte to H_2 exposure are fully reversible, with an extreme change in electrical resistance at 290 °C [14,33]. Higher sensitivities were observed for smaller nanotube diameters. In order to prevent high operating temperatures of the TiO_2 nanotube sensor, the nanotubes were coated with a palladium layer 10 nm thick [15,34,35]. The TiO_2 nanotubes that were synthesized with an aqueous HF electrolyte and coated with Pd film respond to H_2 with a change in electrical resistance of 3 orders of magnitude upon exposure to 1000 ppm H_2 at room temperature [15]. But, the TiO_2 nanotube arrays that were prepared by adding acetic acid to the aqueous HF electrolyte, and by coating fabricated nanotubes with Pd film 10 nm thick respond to 1000 ppm H_2 with a change in electrical resistance of approximately 175 000% at room temperature [34]. On the other hand, the highest sensitivity is observed for 1 μm length TiO_2 nanotube [32]. Thus, the hydrogen sensing properties of TiO_2 nanotube arrays depend on the electrolyte combination, the coating catalyst, the carrier gas, the nanotube length, and the diameter. Similarly, we synthesize TiO_2 nanotube arrays using the aqueous HF electrolyte, and the TiO_2 nanotube arrays are used for hydrogen sensor applications at room temperature without a thin Pd film coating.

In this study, we synthesize highly-ordered TiO_2 nanotubes by anodic oxidation of titanium foil in an aqueous solution containing 1 wt% HF at 20 °C, and investigate their hydrogen sensing properties in terms of the temperature and the hydrogen concentration. The hydrogen sensing mechanism of the TiO_2 nanotubes will be explained in detail.

2. Materials and method

Highly-ordered TiO_2 nanotubes, which are investigated as hydrogen sensors in this work, were grown by the anodization of a commercial pure titanium foil (99%) with a thickness of 0.20 mm. The titanium substrates used as anodic electrodes were mechanically polished with 0.06 μm corn sized colloidal silica suspension (OP-S) and H_2O_2 (30%), electrochemically polished using a solution of 54 mL methanol, 35 mL n-butanol and 6 mL $HClO_4$, and chemically etched in a solution consists of 11.4 mL deionized water, 19.4 mL HNO_3 (70%), 1.417 mL HF (38–40%), to receive a clean and mirror like smooth surface. After every polishing step, the Ti foil is rinsed with deionized water and dried in a nitrogen stream.

The anodization was carried out in an aqueous electrolyte of 1 wt% HF using a DC power supply and a platinum foil as cathode in a thermo-stated bath at a constant temperature of 20 °C. All solutions were prepared from reagent grade chemicals and deionized water (18 MΩ). The distance between the anodic and cathodic electrodes was 20 mm and the total duration of the anodization time was 45 min. Before the experiments, the solutions were stirred using a magnetic stirrer. We used a potential ramp at a rate of 100 $mV\,s^{-1}$ from the open-circuit potential (OCP) to 20 V, and then held this final potential constant during the anodization process. After the anodization, the samples were rinsed in deionized water, dried and characterized. To characterize the morphology, the diameter, and the length of the TiO_2 nanotubes, scanning electron microscopy and energy dispersive X-ray analysis (SEM, Philips XL 30S) were employed with an accelerating voltage of 10 kV. The X-ray diffraction (XRD) was performed on a Philips 1820 X-ray diffractometer with Cu Kα radiation ($\lambda = 1.5418$ Å).

In order to improve the hydrogen (H_2) sensing properties of the anodized TiO_2 nanotubes, the nanotubes were annealed at 500 °C for 3 h in ambient oxygen to obtain crystallized TiO_2 that have both anatase and rutile phases. At this temperature, the walls of the TiO_2 nanotubes adopt an anatase crystal structure, which is necessary to achieve the maximum hydrogen sensitivity [36]. Then the hydrogen sensing measurements were carried out using two platinum pads as electrodes in the temperature range of 20–150 °C. The sensing element was placed in a flow type homemade chamber. The current was measured using a Keithley 6517A Electrometer/High Resistance Meter. During the measurements, the temperature of the sensor was controlled with a Lakeshore 340 temperature controller.

3. Results and discussion

3.1. *Synthesis of titania nanotubes*

We investigate the synthesis of TiO_2 nanotubes by the anodization process using an aqueous electrolyte of 1 wt% HF and H_2 gas sensing properties of these nanotubes array. During the anodization, we continuously record the current through the electrolyte. Fig. 1 shows the current transients ($I-t$ curves) recorded for the constant anodization voltage of 20 V in the aqueous electrolyte of 1 wt% HF. The current decreases rapidly from 400 mA to a few mA in 25 s and then increases to a maximum (110 mA) from this point decreases slowly to a steady-state value (50 mA) in 50 s as seen in Fig. 1. This behavior is in good agreement with the mechanism described below.

The formation of the nanotubes is governed by competition between anodic oxide formation and chemical dissolution of the oxide as soluble fluoride complexes [19].

i) Oxide growth at the surface of the metal due to the interaction of metal with O^{2-} of OH^- ions.

$$2H_2O \rightarrow O_2 + 4e^- + 4H^+ \tag{1}$$

$$Ti + O_2 \rightarrow TiO_2 \tag{2}$$

ii) In the presence of fluoride ions, Ti^{4+} ions arriving at the oxide/solution interface are resolved to TiF_6^{2-}.

$$TiO_2 + 6F^- + 4H^+ \rightarrow TiF_6^{2-} + 2H_2O \tag{3}$$

The current–time graphics can also explain the pore formation process [20].

i) A barrier oxide is formed, leading to a current decay.
ii) The surface is locally activated and pores start to grow randomly. Due to the pore growth the active area increases and the current increases.
iii) The individual pores start interfering with each other, and start competing for the available current and then self-ordering under steady-state conditions is established. The steady-state growth can be characterized by equal rates of TiO_2 dissolution ($v1$) and formation ($v2$).

After the anodization, the samples are characterized by scanning electron microscope (SEM) and energy dispersive X-ray analysis (EDX). Fig. 2a shows the EDX of a typical anodized sample, which is achieved by using the aqueous HF electrolyte. It can be seen that titanium, oxygen, fluorine, and gold are present in the sample. The fluorine and gold come into existence in the EDX analysis because the aqueous HF electrolyte is used for the anodization, and approximately 3 nm thin gold films are coated onto anodized TiO_2 nanotubes with rf sputtering to obtain a conducting surface for SEM analysis. Another typical anodized sample, which is produced similarly, is annealed at 500 °C for 3 h in oxygen ambient. The X-ray diffraction of the sample that was annealed at 500 °C for 3 h in oxygen ambient is shown in Fig. 2b. The labels A, R and T represent the reflections from anatase crystallites, rutile crystallites, and the titanium substrate, respectively. It is clearly seen from Fig. 2b that both the anatase and rutile phases of TiO_2 occur in the sample. Previously, Varghese et al. observed both the anatase and rutile phases of TiO_2 by annealing TiO_2 nanotubes at 500 °C for 6 h in ambient oxygen [14]. At this critical temperature value of 500 °C, the walls of the TiO_2 nanotubes adopt an anatase crystal structure, which is necessary to achieve maximum hydrogen sensitivity, and the barrier layer of the TiO_2 nanotubes adopts a rutile crystal structure [36].

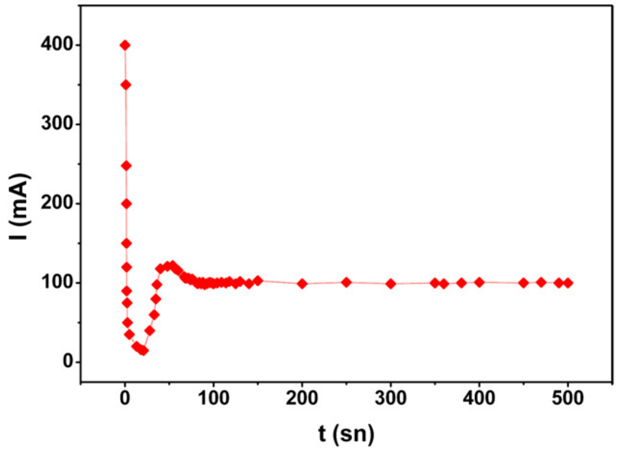

Fig. 1 – $I-t$ curves at a constant potential of 20 V during the anodization process.

While the potential is kept constant during the anodization, the current at the initial stage of oxidation cannot be controlled well. This causes inhomogeneous nucleation and inhomogeneous oxidation. To prevent this uncontrolled growth of oxidation, we use a potential ramp at a rate of 100 mV s^{-1} from the open-circuit potential (OCP) to 20 V, and keep the potential constant at 20 V for 45 min. The SEM images of the TiO_2 nanotubes that are obtained by applying a potential ramp at the initial stage are shown in Fig. 3. The top and cross-sectional views of the nanotube array are shown in Fig. 3a, and the high magnification of the top view is given in Fig. 3b. The TiO_2 nanotube diameter distribution that is obtained from our SEM images is not homogeneous, and it is observed to vary between 40 nm and 110 nm (Fig. 3b). The average diameter of the nanotubes is 90 nm, and the length is approximately 1 μm. In a highly acidic solution, the length of the tubes cannot be increased by prolonging the anodization time. It has previously been reported that for HF containing electrolytes, the TiO_2 nanotubes were grown only up to a length of approximately 500 nm [16,20]. But we synthesize highly-ordered TiO_2 nanotubes with a diameter of 90 nm and a length of 950 nm.

3.2. Hydrogen sensing properties

The hydrogen sensing measurements are carried out using two platinum pads as electrodes in a temperature range 20–150 °C. The sensing element was placed in a flow type homemade chamber. A constant bias voltage of 1 V is applied to the TiO_2 nanotube sensor device, and the change in the DC current is measured upon exposure to 100–5000 ppm H_2 in high purity N_2 at different temperatures. The current values versus time for the TiO_2 nanotube sensor at various temperatures are given in Fig. 4. To establish the baseline, the current is measured under high purity N_2 flow. Then the TiO_2 nanotube sensor is exposed to the desired concentration of H_2 for 100 min and purged with high purity N_2 for 100 min at room temperature (Fig. 4a). The exposing and purging times are 90 min and 60 min at 100 °C and 150 °C, respectively (Fig. 4b and c). The current of the TiO_2 nanotube sensor under high purity N_2 flow is 0.18 nA, 16 nA, and 63 nA at 25 °C, 100 °C, and 150 °C, respectively. This

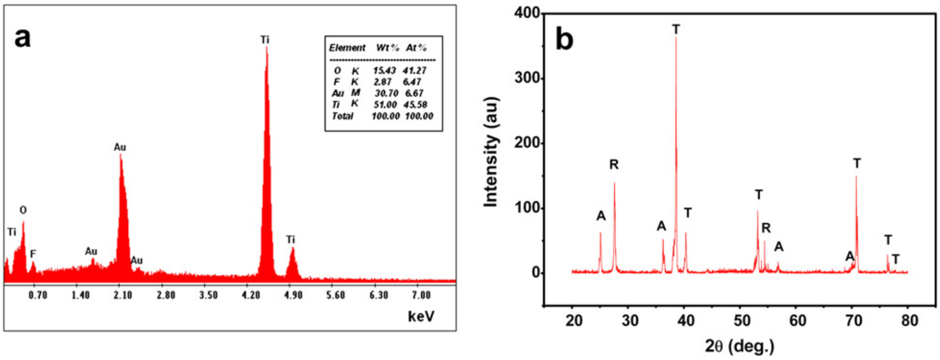

Fig. 2 – a) X-ray diffraction of TiO_2 nanotubes annealed at 500 °C for 3 h in ambient oxygen. The labels A, R, and T represent the reflections from anatase crystallites, rutile crystallites, and the titanium substrate, respectively. b) Energy dispersive X-ray analysis of TiO_2 nanotubes.

increase in the current with increasing temperature is related to the semiconductor behavior of TiO_2. After the sensor is exposed to 100 ppm H_2 at room temperature, the current increases rapidly for 20 min, and then the rate of increase slows down. The current increases from 0.18 nA to 1.91 nA (Fig. 4a). When the H_2 gas is removed by high purity N_2 flow, the recovery appears as a rapid decrease in the current, and then the rate of this decrease gets smaller. However, the current does not come down to its baseline for 100 min. Therefore, the sensor should be purged with high purity N_2 for more than 100 min (Fig. 4a). For the second 100 ppm H_2 and successive H_2 exposures of the sensor, similar behavior is obtained (Fig. 4a). The increase in the current is ascended with increasing concentration of H_2. While the final concentration (5000 ppm) of H_2 is removed with high purity N_2, the full recovery is only achieved in approximately 400 min, as seen in Fig. 4a. In addition, the TiO_2 nanotube sensor is also measured at 100 °C and 150 °C by the same way as we perform the measurements at room temperature. However, the TiO_2 nanotube sensor shows faster full recovery at 100 °C and 150 °C in a shorter time for high purity N_2 purging compared to our results at room temperature, as shown in Fig. 4.

There are four important factors affecting the H_2 sensing properties of TiO_2 nanotubes: catalysis nanofilm coating, carrier gas, nanotube length, and the diameter. Grimes and coworkers synthesized TiO_2 nanotubes with anodization of Ti foil with aqueous HF electrolytes [16], and then investigated the H_2 sensing properties of these nanotubes with two platinum pads at high temperatures [14,33]. They observed an extreme change in the electrical resistance of TiO_2 nanotubes when 1000 ppm H_2 was exposed to the TiO_2 nanotube sensor at 290 °C, and a higher sensitivity for smaller nanotube diameters (22 nm) [14,33]. Yamazoe and Shimanoe have recently developed a new model on the roles of shape and size of component crystals in semiconductor gas sensors on the basis of electron-depleted conditions in component crystals [37,38]. The model confirms that the gas sensitivity increases with decreasing the crystal size and the sensitivity of nanostructured spherical and tubular metal oxide structures is higher than the thin film metal oxide structure.

In order to avoid the high required operating temperature of the TiO_2 nanotube sensor, nanotubes were coated with a 10-nm-thick discontinuous palladium layer using thermal evaporation [15,34,39]. They obtained with a change in the electrical resistance of the TiO_2 nanotube sensor of approximately 4 orders of magnitude in response to 1000 ppm H_2 at room temperature [39]. On the other hand, micrometer-long undoped TiO_2 nanotubes, which were fabricated with anodization using an electrolyte containing potassium fluoride, sodium hydrogen sulfate monohydrate, and sodium citrate tribasic dihydrate, exhibited an unprecedented variation in

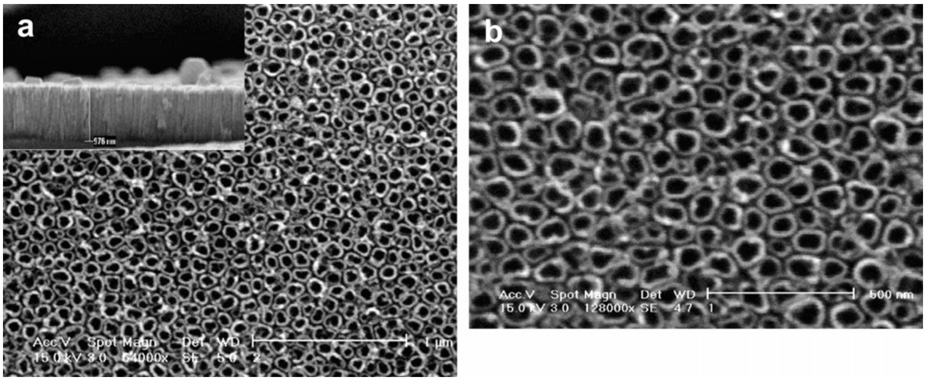

Fig. 3 – SEM images of the top view at different magnifications ((a) 64000× and (b) 128000×) of anodized samples with a ramp rate of 100 mV s^{-1} from the open-circuit potential (OCP) to 20 V and this voltage then held constant. The cross-sectional view of the TiO_2 nanotubes is given in the left-bottom of the top view (a).

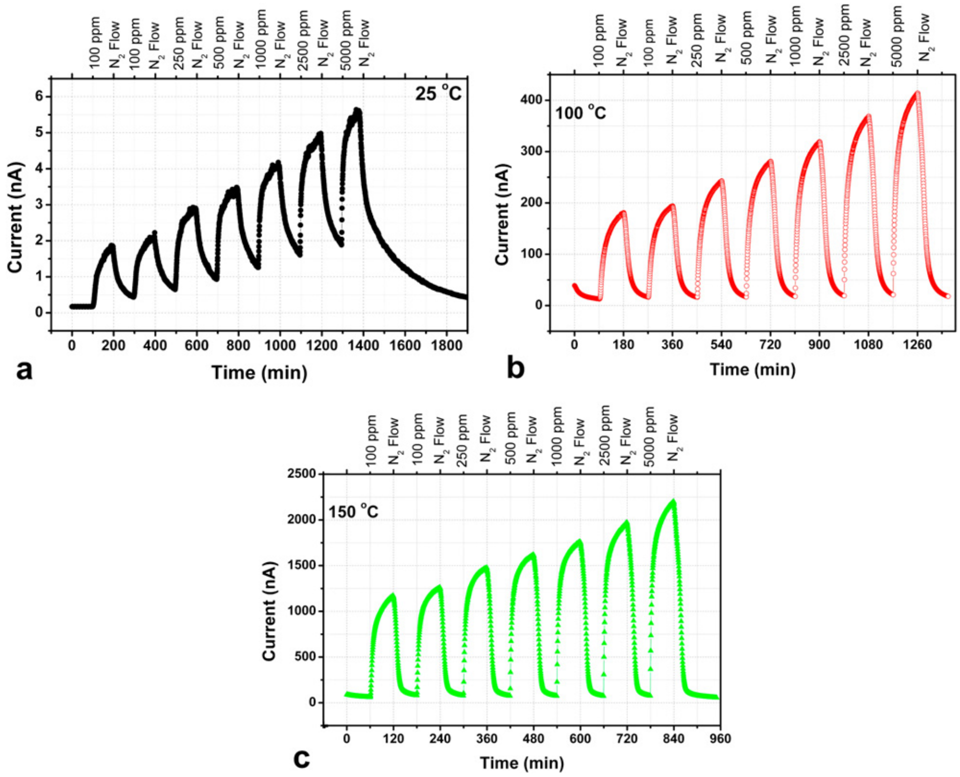

Fig. 4 – Graph of the typical response current versus time for anodized TiO_2 nanotubes exposed to 1 ppm, 1 ppm, 2 ppm, 5 ppm, and 10 ppm H_2 at temperatures of 25 °C (a), 100 °C (b), and 150 °C (c) (the desired times for exposure to H_2 and for purging under dry nitrogen flow are 100 min, 90 min, and 60 min at temperatures of 25 °C (a), 100 °C (b), and 150 °C (c), respectively).

their electrical resistance, of about 8.7 orders of magnitude (50 000 000 000%), at room temperature when exposed to alternating atmospheres of nitrogen containing 1000 ppm hydrogen and air [32]. The highest sensitivity was obtained in the presence of oxygen (with dry air used as the carrier gas) because oxygen in the air was chemisorbed on the nanotube surface, leading to an enhanced base resistance. H_2 then removes this chemisorbed oxygen, thus reducing the resistance [32]. In our case, TiO_2 nanotubes, which were approximately 90 nm in diameter, were fabricated with anodization using aqueous HF electrolyte (1 wt%) and the H_2 sensing properties of these nanotubes without a thin coating of Pd film were in good agreement with previously reported works at the measured temperature interval (25–150 °C). It is observed that the current increases by a factor on the order of approximately 20 when the sensor is exposed to 1000 ppm H_2 at room temperature. This low sensitivity compared to the values recently reported by Grimes and coworkers at room temperature [15,32,34,39] could be explained by the fact that our fabricated TiO_2 nanotubes have larger diameters, no thin Pd film coating is applied, and the sensor is used with N_2 as a carrier gas.

On the other hand, the porous film and nanofiber of TiO_2 without catalysis film coating were used for H_2 sensor at high temperature (above 250 °C) [40,41]. Mukherjee et al. found that the titanium film coated porous TiO_2 was less sensitive to 500 ppm hydrogen in air ambient below 300 °C [40]. They obtained the sensitivity of porous TiO_2 approximately 1 for sample anodized at 50 mA cm^{-2} in 1 M sulphuric acid when 500 ppm hydrogen exposed to the sensor. In addition, Seo et al. observed the sensitivity of TiO_2 nanotubes' exposure to 500 ppm hydrogen as approximately 10 without catalysis film coating at above 450 °C [42]. They fabricated TiO_2 nanotubes by a hydrothermal treatment of TiO_2 nanoparticles in a NaOH solution at the different temperatures. In our case the Pt pad is played a crucial rule to use TiO_2 nanotubes as a sensitive material at room temperature for hydrogen sensor.

The H_2 sensing mechanism of TiO_2 nanotubes is explained by a variety of factors. The primary factor in the interaction between the nanotubes and hydrogen is the chemisorption of the dissociated hydrogen on the TiO_2 surface [43]. The electrical conductivity of TiO_2 nanotubes is enhanced when the chemisorbed hydrogen acts in the surface states of the nanotubes. The chemisorption of hydrogen onto the walls and intertubular connecting points could cause easy charge transfer with less resistance in tube to tube transfers. Another factor is that the platinum electrode pads may play a role in the hydrogen absorption. It is well known that platinum is a catalyst for hydrogen. Thus, hydrogen can dissociate on platinum surfaces. These dissociated hydrogen atoms may spill onto the nanotube surface, where they diffuse into the nanotube surface [43–45]. Another factor is that anatase, the polymorph of TiO_2, has been reported to be of high sensitivity toward reducing gases like hydrogen and carbon monoxide [46]. The hydrogen diffused to the interstitial sites of TiO_2. The c/a ratio of anatase is almost four times that of the normal rutile, so the anatase phase of TiO_2 has a greater contribution to hydrogen sensitivity. At the critical temperature of 500 °C, the walls of the TiO_2 nanotubes adopt an anatase crystal structure, which is necessary to achieve maximum hydrogen sensitivity, and the barrier layer of the TiO_2 nanotubes adopts a rutile crystal structure [36]. In our case, the mechanism of the H_2 sensor is made up of only undoped TiO_2 nanotubes annealed at 500 °C for 3 h. The only reason for the low sensitivity is the chemisorption of H_2.

In order to compare the response times, the parameter t_{90} was defined as the time it takes for the sensor signal to reach 90% of its saturation value. The response time (t_{90}) of the TiO_2 nanotube sensor is 65 min at room temperature and decreases to 30 min with increasing temperatures. The diffusivity of the H atoms increases rapidly with increasing temperature, causing a decreasing response time (t_{90}). This higher response time is related to the chemisorption of H_2 on the TiO_2 nanotube sensor. On the other hand, the sensitivity is defined as

$$S = \frac{I_g - I_0}{I_0}, \tag{4}$$

where I_g is the current after the sensor is exposed to H_2, and I_0 is the reference value of the sensor device exposed to high purity N_2. Fig. 5 shows the sensitivity versus time when the TiO_2 nanotube sensor is exposed to 100 ppm H_2 at different temperatures. The sensitivity increases from 10 to 18 with increasing temperatures under exposure to 100 ppm H_2.

Fig. 6 shows the sensitivity versus the concentration of H_2 for the TiO_2 nanotube sensor at desired temperatures. A nonlinear relationship, which could be related to Langmuir isotherms, between the sensitivity and concentration was obtained for all temperatures. Previously, the concentration dependent sensitivity of the TiO_2 nanotubes for H_2 sensors was well represented by Langmuir isotherms [33]. The dependence of the sensitivity on the H_2 concentration is nearly linear at low concentrations, and the sensitivity appeared to saturate for high concentrations above 1000 ppm H_2 at the desired temperatures. The sensitivity increases from 17 to 28 for 1000 ppm H_2 with increasing temperatures, and the highest sensitivity is observed at 150 °C.

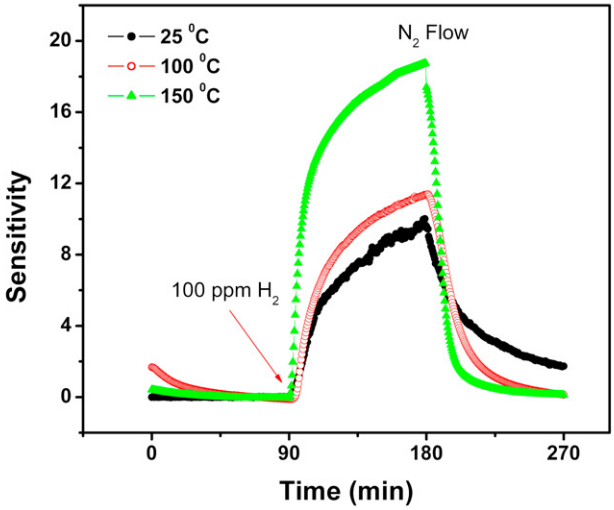

Fig. 5 – Graph of sensitivity versus time for anodized TiO_2 nanotubes at temperatures of 25 °C, 100 °C, and 150 °C while exposed to 100 ppm H_2.

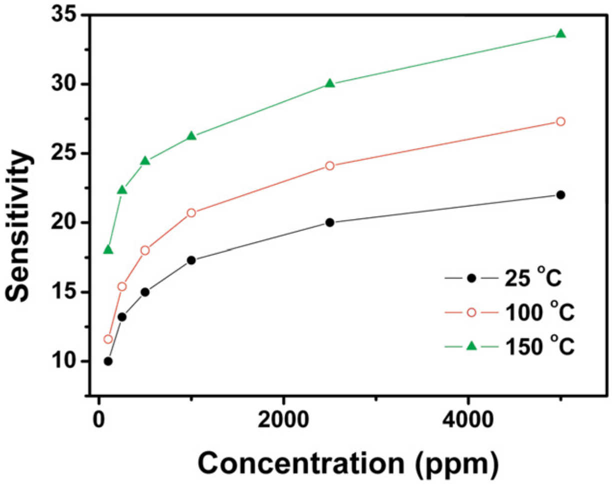

Fig. 6 – Graph of sensitivity versus concentration of hydrogen at temperatures of 25 °C, 100 °C, and 150 °C for anodized TiO_2 nanotubes.

4. Conclusions

Vertically oriented TiO_2 nanotube arrays that are approximately 1 μm in length and 90 nm in pore diameter are fabricated with the anodization method using an aqueous HF electrolyte (1 wt%) at a 20 °C anodization temperature. Our TiO_2 nanotubes are observed to be longer than those in previous reports that also used aqueous HF electrolytes. This could be related to our use of a potential ramp at a rate of 100 mV s^{-1} from the open-circuit potential (OCP) to 20 V, followed by holding this final potential constant. The fabricated TiO_2 nanotubes are annealed in a dry air atmosphere at 500 °C for 3 h to obtain high sensitivity to hydrogen. The hydrogen sensitivity of the synthesized nanotubes increases nearly tenfold, from 10 to 18, with increasing temperature (25–150 °C) for 100 ppm H_2. In summary, it was demonstrated that TiO_2 nanotube sensors that are prepared using anodization can successfully be used as hydrogen sensors at low temperatures.

Acknowledgements

This work has been funded by The Scientific and Technological Research Council of Turkey (TUBİTAK), Project Number: 106T546.

REFERENCES

[1] Bevenot X, Trouillet A, Veillas C, Gagnaire H, Clement M. Hydrogen leak detection using an optical fibre sensor for

aerospace applications. Sensors and Actuators B: Chemical 2000;67:57–67.
[2] Yazdi N, Ayazi F, Najafi K. Micromachined inertial sensors. Proceedings of the IEEE 1998;86:1640–59.
[3] Katsuki A, Fukui K. H-2 selective gas sensor based on SnO_2. Sensors and Actuators B: Chemical 1998;52:30–7.
[4] Boon-Bretta L, Bousek J, Moretto P. Reliability of commercially available hydrogen sensors for detection of hydrogen at critical concentrations: part II – selected sensor test results. International Journal of Hydrogen Energy 2009; 34:562–71.
[5] Taşaltın N, Öztürk S, Kılınç N, Öztürk ZZ. Temperature dependence of a nanoporous Pd film hydrogen sensor based on an AAO template on Si. Applied Physics A: Materials Science & Processing 2009;97:745–50.
[6] Christofides C, Mandelis A. Solid-state sensors for trace hydrogen gas-detection. Journal of Applied Physics 1990;68: R1–30.
[7] Ruths PF, Ashok S, Fonash SJ. A study of Pd–Si MIS Schottky-barrier diode hydrogen detector. IEEE Transactions on Electron Devices 1981;28:1003–9.
[8] Taşaltın N, Dumludağ F, Ebeoğlu MA, Yüzer H, Öztürk ZZ. Pd/native nitride/n-GaAs structures as hydrogen sensors. Sensors and Actuators B: Chemical 2008;130:59–64.
[9] Aroutiounian V. Metal oxide hydrogen, oxygen, and carbon monoxide sensors for hydrogen setups and cells. International Journal of Hydrogen Energy 2007;32:1145–58.
[10] Adamyan AZ, Adamyan ZN, Aroutiounian VM. Study of sensitivity and response kinetics changes for SnO_2 thin-film hydrogen sensors. International Journal of Hydrogen Energy 2009;34:8438–43.
[11] Chiua SY, Huanga HW, Huanga TH, Lianga KC, Liua KP, Tsaib JH, et al. Comprehensive investigation on planar type of Pd–GaN hydrogen sensors. International Journal of Hydrogen Energy 2009;34:5604–15.
[12] Savage N, Chwieroth B, Ginwalla A, Patton BR, Akbar SA, Dutta PK. Composite n–p semiconducting titanium oxides as gas sensors. Sensors and Actuators B: Chemical 2001;79:17–27.
[13] Miyazaki H, Hyodo T, Shimizu Y, Egashira M. Hydrogen-sensing properties of anodically oxidized TiO_2 film sensors: effects of preparation and pretreatment conditions. Sensors and Actuators B: Chemical 2005;108:467–72.
[14] Varghese OK, Gong D, Paulose M, Ong KG, Grimes CA. Hydrogen sensing using titania nanotubes. Sensors and Actuators B: Chemical 2003;93:338–44.
[15] Mor GK, Varghese OK, Paulose M, Grimes CA. A self-cleaning, room-temperature titania-nanotube hydrogen gas sensor. Sensor Letters 2003;1:42–6.
[16] Gong D, Grimes CA, Varghese OK, Hu W, Singh RS, Chen Z, et al. Titanium oxide nanotube arrays prepared by anodic oxidation. Journal of Materials Research 2001;16:3331–4.
[17] Mor GK, Varghese OK, Paulose M, Mukherjee N, Grimes CA. Fabrication of tapered, conical-shaped titania nanotubes. Journal of Materials Research 2003;18:2588–93.
[18] Cai Q, Paulose M, Varghese OK, Grimes CA. The effect of electrolyte composition on the fabrication of self-organized titanium oxide nanotube arrays by anodic oxidation. Journal of Materials Research 2005;20:230–6.
[19] Mor GK, Shankar K, Paulose M, Varghese OK, Grimes CA. Enhanced photocleavage of water using titania nanotube arrays. Nano Letters 2005;5:191–5.
[20] Lee WJ, Alhoshan M, Smyrl WH. Titanium dioxide nanotube arrays fabricated by anodizing processes – electrochemical properties. Journal of the Electrochemical Society 2006;153: 499–505.
[21] Beranek R, Hildebrand H, Schmuki P. Self-organized porous titanium oxide prepared in H_2SO_4/HF electrolytes. Electrochemical and Solid-State Letters 2003;6:12–4.
[22] Tian T, Xiao XF, Liu RF. Study on titania nanotube arrays prepared by titanium anodization in NH_4F/H_2SO_4 solution. Journal of Materials Science 2007;42:5539–43.
[23] Macak JM, Tsuchiya H, Schmuki P. High-aspect-ratio TiO_2 nanotubes by anodization of titanium. Angewandte Chemie International Edition 2005;44:2100–2.
[24] Allam NK, Grimes CA. Formation of vertically oriented TiO_2 nanotube arrays using a fluoride free HCl aqueous electrolyte. Journal of Physical Chemistry C 2007;111: 13028–32.
[25] Yoriya S, Prakasam HE, Varghese OK, Shankar K, Paulose M, Mor GK, et al. Initial studies on the hydrogen gas sensing properties of highly-ordered high aspect ratio TiO_2 nanotube-arrays 20 μm to 222 μm in length. Sensor Letters 2006;4:334–9.
[26] Albu SP, Ghicov A, Macak JM, Schmuki P. 250 μm long anodic TiO_2 nanotubes with hexagonal self-ordering. Physica Status Solidi – Rapid Research Letters 2007;1:65–7.
[27] Paulose M, Prakasam HE, Varghese OK, Peng L, Popat KC, Mor GK, et al. TiO_2 nanotube arrays of 1000 μm length by anodization of titanium foil: phenol red diffusion. Journal of Physical Chemistry C 2007;111:14992–7.
[28] Mahajana VK, Mohapatraa SK, Misra M. Stability of TiO_2 nanotube arrays in photoelectrochemical studies. International Journal of Hydrogen Energy 2008;33: 5369–74.
[29] Ghicov A, Schmuki P. Self-ordering electrochemistry: a review on growth and functionality of TiO_2 nanotubes and other self-aligned MO_x structures. Chemical Communications 2009;20:2791–808.
[30] Macak JM, Tsuchiya H, Ghicov A, Yasuda K, Hahn R, Bauer S, et al. TiO_2 nanotubes: self-organized electrochemical formation, properties and applications. Current Opinion in Solid State and Materials Science 2007;11:3–18.
[31] Mor GK, Varghese OK, Paulose M, Shankar K, Grimes CA. A review on highly ordered vertically oriented TiO_2 nanotube arrays: fabrication, material properties, and solar energy applications. Solar Energy Materials and Solar Cells 2006;90: 2011–75.
[32] Paulose M, Varghese OK, Mor GK, Grimes CA, Ong KG. Unprecedented ultra-high hydrogen gas sensitivity in undoped titania nanotubes. Nanotechnology 2006;17:398–402.
[33] Varghese OK, Gong DW, Paulose M, Ong KG, Dickey EC, Grimes CA. Extreme changes in the electrical resistance of titania nanotubes with hydrogen exposure. Advanced Materials 2003;15:624–7.
[34] Mor GK, Carvalho MA, Varghese OK, Pishko MV, Grimes CA. A room-temperature TiO_2-nanotube hydrogen sensor able to self-clean photoactively from environmental contamination. Journal of Materials Research 2004;19:628–34.
[35] Varghese OK, Mor GK, Grimes CA, Paulose M, Mukherjee N. A titania nanotube-array room-temperature sensor for selective detection of hydrogen at low concentrations. Journal of Nanoscience and Nanotechnology 2004;4:733–7.
[36] Varghese OK, Gong DW, Paulose M, Grimes CA, Dickey EC. Crystallization and high-temperature structural stability of titanium oxide nanotube arrays. Journal of Materials Research 2003;18:156–65.
[37] Yamazoe N, Shimanoe K. Roles of shape and size of component crystals in semiconductor gas sensors I. Response to oxygen. Journal of the Electrochemical Society 2008;155:J85–92.
[38] Yamazoe N, Shimanoe K. Receptor function and response of semiconductor gas sensor. Journal of Sensors; 2009:1–21. 875704.
[39] Mor GK, Varghese OK, Paulose M, Ong KG, Grimes CA. Fabrication of hydrogen sensors with transparent titanium

oxide nanotube-array thin films as sensing elements. Thin Solid Films 2006;496:42–8.

[40] Mukherjee T, Hazra SK, Basu S. Porous titania thin films grown by anodic oxidation for hydrogen sensors. Materials and Manufacturing Processes 2006;21:247–51.

[41] Yoo S, Akbar SA, Sandhage KH. Nanocarving of titania (TiO_2) a novel approach for fabricating chemical sensing platform. Ceramics International 2004;30:1121–6.

[42] Seo MH, Yuasa M, Kida T, Huh JS, Shimanoe K, Yamazoe N. Gas sensing characteristics and porosity control of nanostructured films composed of TiO_2 nanotubes. Sensors and Actuators B: Chemical 2009;137:513–20.

[43] Raupp GB, Dumesic JA. Adsorption of CO, CO_2, H_2 and H_2O on titania surfaces with different oxidation states. Journal Physical Chemistry 1985;89:5240–6.

[44] Madou MJ, Morrison SR. Chemical sensing with solid state devices. New York: Academic Press; 1989.

[45] Roland U, Braunschweig T, Roessner F. On the nature of split-over hydrogen. Journal of Molecular Catalysis A: Chemical 1997;127:61–84.

[46] Birkefeld LD, Azad AM, Akbar SA. Carbon monoxide and hydrogen detection by anatase modification of titanium dioxide. Journal of the American Ceramic Society 1992;75: 2964–8.